Global Change Biology

Global Change Biology (2012) **18**, 1769–1780, doi: 10.1111/j.1365-2486.2012.02648.x

Modeling biophysical controls on canopy foliage water ^{18}O enrichment in wheat and corn

WEI XIAO*, XUHUI LEE†, XUEFA WEN‡, XIAOMIN SUN‡ and SHICHUN ZHANG§

*Key Laboratory of Meteorological Disaster of Ministry of Education & Yale-NUIST Center on Atmospheric Environment, Nanjing University of Information Science & Technology, Nanjing, 210044, China, †School of Forestry and Environmental Studies, Yale University, New Haven, Connecticut 06511, USA, ‡Institute of Geographic Sciences and Natural Resources Research, Chinese Academy of Sciences, Beijing, 100101, China, §Northeast Institute of Geography and Agroecology, Chinese Academy of Sciences, Changchun, 130012, China

Abstract

Leaf water ^{18}O enrichment is an important factor controlling the $H_2{}^{18}O$, $C^{18}OO$, and $O^{18}O$ exchanges between the biosphere and the atmosphere. At present, there is limited capacity to explain the enrichment mechanisms in field conditions. In this study, three models of varying complexity were used to simulate the leaf water ^{18}O enrichment at the canopy scale. Comparisons were made among the models and with high-frequency isotopic measurements of ecosystem water pools in wheat and corn. The results show that the steady state assumption was a better approximation for ecosystems with lower canopy resistance, that it is important to consider the effect of leaf water turnover in modeling the enrichment and not necessary to deal with time changes in leaf water content, and that the leaf-scale Péclet effect was incompatible with the big-leaf modeling framework for canopy-air interactions. After turbulent diffusion has been accounted for in an apparent kinetic factor parameterization, the mean ^{18}O composition of the canopy foliage water was a well-behaved property predictable according to the principles established by leaf-scale studies, despite substantial variations in the leaf water enrichment with leaf and canopy positions. In the online supplement we provided a discussion on the observed variability of leaf water ^{18}O composition with leaf and canopy positions and on the procedure for correcting isotopic measurements for organic contamination.

Keywords: biophysical factors, canopy scale, corn, foliage water ^{18}O enrichment, model, wheat

Received 5 December 2011; revised version received 5 December 2011 and accepted 31 December 2011

Introduction

In the process of transpiration, leaf water of terrestrial plants is more enriched in ^{18}O than the water taken up by their roots, due to the slower diffusion (the kinetic effect) through the stomatal opening and the lower saturation vapor pressure (the equilibrium effect) of the heavier $H_2{}^{18}O$ molecules than the lighter $H_2{}^{16}O$ molecules. The enriched ^{18}O signal is an important factor controlling the $H_2{}^{18}O$, $C^{18}OO$ and $O^{18}O$ exchanges between the biosphere and the atmosphere and insights into its biophysical controls are highly relevant to issues of interest to biologists and global change scientists. The ^{18}O tracer provides unique constraints on water and carbon cycles (Farquhar *et al.*, 1993, 2007; Yakir *et al.*, 1994), paleoclimate reconstruction (Gray & Thompson, 1976; Libby Pandolfi *et al.*, 1976; Epstein & Yapp, 1977; Roden *et al.*, 2000; Cullen *et al.*, 2008) and the Earth's Dole effect (Dole *et al.*, 1954; Bender *et al.*, 1994; Hoffmann *et al.*, 2004). During terrestrial photosynthesis, some of the CO_2 entering chloroplasts is assimilated after having exchanged oxygen atoms with the ^{18}O-enriched water, a process that transfers the leaf water ^{18}O signal to plant materials (Farquhar *et al.*, 1993). In recent years, an active area of research in global change concerns the ^{18}O content in plant biomarkers as proxies of environmental conditions influencing the plant growth (Barbour *et al.*, 2000; Evans & Schrag, 2004; Miller *et al.*, 2006; Treydte *et al.*, 2006; Barbour, 2007; Helliker & Richter, 2008; Sternberg, 2009; Kahmen *et al.*, 2011). Central to these and other related studies is a mechanistic understanding on how biotic and abiotic factors influence the leaf water $^{18}O/^{16}O$ ratio (δ_L, in delta notation in reference to VSMOW).

A distinction should be made between leaf- and canopy-scale processes. The mechanistic models for foliage water ^{18}O enrichment, reviewed below, are constructed at the leaf scale, requiring input variables measured

Correspondence: Dr. Xuhui Lee, School of Forestry and Environmental Studies, Yale University, 21 Sachem Street, New Haven, Connecticut 06510, USA, tel. + 1 203 432 6271, fax + 1 203 432 5023, e-mail: xuhui.lee@yale.edu; Dr. Xuefa Wen, Institute of Geographic Sciences and Natural Resources Research, Chinese Academy of Sciences, A11 Datun Road, Chaoyang District, Beijing 100101, China, tel. + 86 10 64 889 432, fax + 86 10 64 889 399, e-mail: wenxf@igsnrr.ac.cn

immediately outside the leaf boundary layer. The above-mentioned applications, on the other hand, relate the enrichment to environmental conditions occurring outside the plant canopy, in the so-called atmospheric surface layer, and in this context, the appropriate modeling framework should be aimed at the canopy scale. Similarly, knowledge of the canopy scale ^{18}O enrichment is a prerequisite for flux partitioning studies involving the $C^{18}OO$ and $H_2{}^{18}O$ tracers (Ogée *et al*., 2004; Lee *et al*., 2007). By providing the lower boundary conditions for global modeling systems of atmospheric $H_2{}^{18}O$, $C^{18}OO$ and $O^{18}O$ (Farquhar *et al*., 1993; Ciais *et al*., 1997; Riley *et al*., 2002; Cuntz *et al*., 2003; Hoffmann *et al*., 2004), models of the ^{18}O leaf enrichment at the canopy scale help to bridge field research, which generates local empirical knowledge, and a mechanistic understanding of the changes of these isotopologues in the atmosphere at the global scale.

Mathematical models for predicting δ_L are built on our understanding of fractionations associated with phase change of water during transpiration. The first model of the evaporative enrichment was based on the theory developed by Craig & Gordon (1965, referred to as C65 hereafter) and calculates δ_L with the assumptions of isotopic homogeneity in leaf water and the steady state, the latter of which states that the isotopic concentration of water entering the leaf equals that leaving the leaf. Dongmann *et al*. (1974, D74) employed C65 to calculate δ_L in non-steady state and retained the assumption that ^{18}O is evenly distributed in the leaf water pool. In the non-steady state model of Farquhar & Cernusak (2005, F05), biotic controls are included by considering the heterogeneous isotopic composition of leaf water and temporal variations of leaf water content (W). Ogée *et al*. (2007) developed a two-dimensional model for non-steady state and associated the microscale spatial patterns of isotopic enrichment in the leaf with leaf geometry and nonuniform gas exchange parameters. Few studies have evaluated these models over full growing seasons and in field conditions (Wingate *et al*., 2010; Xiao *et al*., 2010; Griffis *et al*., 2011).

The goal of this modeling study is to evaluate the performance of the models C65, D74, and F05 against observations made in wheat and corn. Plant materials were collected at high temporal frequencies and in spatial replicates to characterize the canopy-scale δ_L. Data of this kind are rare because such a destructive sampling scheme may not be acceptable for natural ecosystems. As two major food crops, the areas of wheat and corn are over 31 and 24 million ha in China and over 230 and 160 million ha worldwide, respectively, according to the Food and Agriculture Organization of the United Nation, and represent two different photosynthetic modes (C_3 and C_4, respectively). Previous studies have shown that species with parallel vein structures, such as grasses, display much larger variations in δ_L with leaf position than species with reticulate venation such as cotton (Yakir *et al*., 1994; Wang & Yakir, 1995; Helliker & Ehleringer, 2000; Gan *et al*., 2002, 2003). Having parallel vein structures, wheat and corn may be good model systems for grassland ecosystems. By comparing the three models of varying complexity, we wish to quantify the influences of the Péclet effect, non-steady state and changes in leaf water content on the ^{18}O enrichment at the canopy scale. We will investigate biotic (such as stomatal behavior and leaf water content) and abiotic controls (such as relative humidity and air turbulence) on the isotopic enrichment. Finally, we will test the hypothesis that despite substantial variations in δ_L with leaf and canopy positions (Appendix A, Online Supplement), the mean $\delta^{18}O$ of foliage water at the canopy scale is a well-behaved property predictable according to the simple big-leaf model of biosphere-atmosphere interactions. In Appendix A, we present an analysis of the spatial variations with leaf position and canopy position observed in the wheat and corn experiments.

Materials and methods

Site and Data

The experiment was conducted at the Luancheng Agro-Ecosystem Experimental Station (37° 53′ N, 114° 41′ E, elevation 50 m), located in the North China Plain (Wen *et al*., 2012). Wheat (*Triticum aestivum* L.) was planted in November of 2007 and harvested on June 18, 2008 (day of year or DOY 170), with a maximum LAI of 4.5 and a maximum height of 0.75 m observed on DOY 120. Corn (*Zea mays* L.) was planted in the beginning of June before wheat harvest, with a maximum LAI of 4.2 and a maximum height of 2.77 m reached on August 16 (DOY 229). The wheat and corn cultivation was 16 ha in size. The fetch of the measurement site was greater than 200 m.

Isotopic measurements were made of ecosystem water pools. The O^{18}/O^{16} ratio in water vapor was measured continuously using a tunable diode laser (TDL) trace gas analyzer (Model TGA100A; Campbell Scientific Inc., Utah, USA; Wen *et al*., 2012). Air was sampled at two heights above the canopy; they were increased from 0.6/1.6 m at the beginning to 1.1/2.1 m at the end of the wheat season and from 1.1/2.1 m at the beginning to 3.2/4.2 m at the end of the corn season, to adjust for plant growth. In this study, the measurement at the lower intake was used. Leaf, stem and soil samples were collected from four sampling plots within 50 m of the gas intakes. Leaf samples from the upper and lower canopy were archived separately, with the main leaf vein removed. In the case of corn, the leaf samples were a mixture of small sections from the upper, middle and bottom positions of the leaf. Soil samples were collected from the depths of 0–5, 15–20 and 40–45 cm. Water in these solid samples was extracted using a

vacuum extraction system (West *et al*., 2006). Precipitation and dew water were also collected on an event-by-event basis. Precipitation was collected using an open container with mineral oil inside to block evaporation. During dew events, dew water was removed before dawn from the leaf surface using clean cotton balls and squeezed to sampling vials (Wen *et al*., 2012). Isotopic composition of the liquid water was measured with an isotopic ratio infrared spectroscopy (IRIS, Model DLT-100; Los Gatos Research, Mountain View, CA, USA) and corrected for organic contaminants following the procedure of Schultz *et al*. (2011). The average correction was 2.5‰ for leaf water samples and 1.1‰ for stem water samples. A subset of the leaf water samples was also measured with an isotope ratio mass spectrometer (IRMS, MAT 253; Finnigan Inc.) using a continuous flow method. The mean difference (standard deviation) between the IRIS and the IRMS measurements was −0.3‰ (±0.7‰, number of samples = 163). More details on the IRIS correction procedure are given in Appendix B.

For most of the experiment, collection of leaf, stem, and soil samples was made at midday between 12:00 and 14:00 LST every 2–4 days. On several days, additional collection was made at 06:00 and 18:00 LST. During four intensive periods (DOY 134-137, 142-144, 236-237, and 244-246), the samples were collected every 3–4 h. On DOY 256, five segments from the base to the tip of 4 corn leaves were sampled every 3 h from 6:00 to 18:00 LST.

Leaf water content (W, mol m^{-2} leaf area) was measured at the same time of leaf sampling. For the canopy-scale model simulations, the canopy foliage water content was computed as the product of W and LAI, in units of mol m^{-2} (ground area).

Supporting canopy-scale measurements included eddy covariance fluxes and routine meteorological variables. The latent heat, sensible heat, momentum, and CO_2 fluxes were measured using a sonic anemometer (CSAT-3; Campbell Scientific Inc.) and a CO_2/H_2O infrared analyzer (LI-7500; Licor Inc., Lincoln, NB, USA) which were mounted at a 3-m height above the ground. Soil heat flux was measured at a depth of 2 cm with three heat flux sensors (HFP01; Campbell Scientific Inc.). Air temperature and humidity (HMP45C; Campbell Scientific Inc.), and wind speed (A100R; Vector Instruments, Rhyl, North Wales, UK) were measured at 1.4 m and 3.9 m heights. Net radiation was measured with a 4-component radiometer (CNR-1; Kipp & Zone, Delft, The Netherlands). Canopy temperature was measured with an infrared radiometer (IRTS-P; Apogee Instruments Inc., Logan, UT, USA). Soil temperature was measured using thermocouples (105T; Campbell Scientific Inc.) at 10, 20, and 50 cm depths. Soil water content was measured with water content reflectometers (CS616-L; Campbell Scientific Inc.) at 5, 20, and 50 cm depths. Precipitation was measured with a rain gauge (TE525MM; Campbell Scientific Inc.).

During the intensive periods, physiological measurement was conducted simultaneously with the leaf and stem sampling using a photosynthesis system (LI-6400; Licor Inc.). Stomatal resistance, transpiration, photosynthesis, leaf temperature (T_L), and vapor pressure deficit (VPD) were measured at the same canopy positions of leaf sampling.

Models

Overall Model Structure. The simple isotopic land surface model (SiLSM) of Xiao *et al*. (2010) was modified here to simulate the $H_2{}^{18}O$ composition of foliage water. SiLSM was originally developed to simulate the isotopic exchanges of $H_2{}^{18}O$ and $C^{18}OO$ between ecosystems and the atmosphere. It consists of three submodels, i.e., a parameterization of the $C^{18}OO$ isoforcing, a submodel for $H_2{}^{18}O$ enrichment in foliage water and a big-leaf land surface model. In this article, the latter two submodels were employed. The $H_2{}^{18}O$ submodel of SiLSM is adopted from Farquhar & Cernusak (2005, F05). In this study, we also evaluated the performance of the leaf water enrichment submodels of Craig & Gordon (1965, C65) and Dongmann *et al*. (1974, D74). Fig. 1 shows the overall model structures, and Table 1 summarizes the key assumptions made by these isotope submodels. A detailed description of these modeling components is provided below.

Isotopic Leaf Enrichment Submodels. The C65 submodel was originally developed to calculate the isotopic composition of evaporation water vapor from a liquid water surface, as

$$\delta_E = [\alpha_{eq}\delta_L - h\delta_a - \varepsilon_{eq} - (1-h)\varepsilon_k]/[(1-h) + (1-h)\varepsilon_k/1000] \quad (1)$$

where subscripts E, L, and a represent the evaporating water vapor, liquid water body and atmospheric water vapor, respectively, α_{eq} (>1) is the equilibrium fractionation factor (Majoube, 1971), $\varepsilon_{eq} = (1 - 1/\alpha_{eq})1000$, ε_k is the kinetic fractionation factor, and h is the relative humidity of the ambient air referenced to the water surface temperature. This model is used to predict the leaf water enrichment (Dongmann *et al*., 1974; Bariac *et al*., 1989; Walker *et al*., 1989; Flanagan & Ehleringer, 1991; Flanagan *et al*., 1991). With the assumptions that the leaf water is isotopically well mixed (that is, $\delta_{L,b} = \delta_{L,e}$, where $\delta_{L,b}$ is the ^{18}O composition of bulk leaf water and $\delta_{L,e}$ is that at the evaporating site in the leaf) and that transpiration is in isotopic steady state (that is, $\delta_x = \delta_E$), we obtain

$$\delta^s_{L,b} = \delta_x + \varepsilon_{eq} + \varepsilon_k + h(\delta_a - \varepsilon_k - \delta_x) \quad (2)$$

where superscript s denotes the steady state prediction, and subscript x represents xylem water. In the canopy-scale

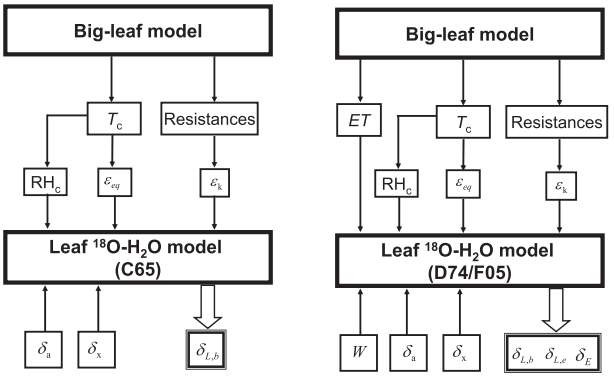

Fig. 1 Schematic diagram of the model structures.

Table 1 Description of the isotopic submodels

Models	*W* variation	Non-steady state	Péclet effect
Craig & Gordon (C65)	No	No	No
Dongmann *et al.* (D74)	No	Yes	No
Farquhar and Cernusak (F05)	Yes	Yes	Yes

application, $\delta_{L,b}$ is the mean foliage ^{18}O composition of the canopy layer, ε_{eq} and h are in reference to the canopy temperature T_c, δ_a is the ^{18}O composition of water vapor in the surface layer over the canopy, and ε_k is the canopy apparent kinetic fractionation factor given as

$$\varepsilon_k = \frac{28r_c + 19r_b}{r_a + r_b + r_c} \tag{3}$$

where r_a, r_b, and r_c are aerodynamic, boundary layer and canopy resistance, respectively. In this formulation, the molecular kinetic factor (28‰) and the kinetic factor associated with the leaf boundary layer (19‰) are given by Merlivat (1978) and Farquhar *et al.* (1989), respectively, and no fractionation occurs in turbulent diffusion in the atmospheric surface layer (Lee *et al.*, 2009).

Numerous modeling and experimental studies have shown that the assumption of steady state is not fulfilled in field conditions (e.g., Dongmann *et al.*, 1974; Cernusak *et al.*, 2005; Farquhar & Cernusak, 2005; Lai *et al.*, 2006; Welp *et al.*, 2008). D74 expresses the isotopic enrichment of leaf water in non-steady state, as

$$\frac{d\delta_{L,b}}{dt} = -\frac{w_i}{Wr_t\alpha_k\alpha_{eq}}(\delta_{L,b} - \delta^s_{L,b}) \tag{4}$$

where $\delta^s_{L,b}$ and $\delta_{L,b}$ are the ^{18}O composite of bulk leaf water in steady and non-steady state, respectively, w_i is the mole fraction of water vapor in the intercellular space, W is the leaf water content, r_t is total resistance to the diffusion of water vapor, α_k is the fractionation factor for diffusion ($\alpha_k = 1 + \varepsilon_k/1000$). The solution of Eqn (4) at time t is

$$\delta_{L,b} = \delta^s_{L,b} + [\delta^0_{L,b} - \delta^s_{L,b}]e^{-t/\tau} \tag{5}$$

where $\delta^0_{L,b}$ is $\delta_{L,b}$ at time zero, and τ is a time constant given by

$$\tau = \frac{Wr_t\alpha_k\alpha_{eq}}{w_i} \tag{6}$$

In the canopy-scale framework, W is the canopy water content per unit ground area (mol m^{-2}). D74 makes two implicit assumptions. As with C65, it assumes that the leaf water is well mixed. In addition, W is taken as a constant invariant with time (White, 1989).

In F05, no assumption is made about steady state, a well mixed leaf water pool, or a constant W. Leaf-scale measurements have shown that leaf water is not isotopically well mixed; its ^{18}O composition is highest at the evaporation site in the leaf and lowest near the xylem (Helliker & Ehleringer, 2000; Yakir & Sternberg, 2000; Gan *et al.*, 2002). The progressive enrichment from the xylem to the site of evaporation maintains an isotopic gradient that drives the diffusion of $H_2{}^{18}O$ molecules in the opposite direction of mass water flow in the leaf, a phenomenon termed the Péclet effect (Farquhar & Lloyd, 1993). The F05 submodel has taken the Péclet effect into account. The key equations of F05 are

$$\delta_{L,b} = \delta^s_{L,b} - \frac{\alpha_k\alpha_{eq}r_t}{w_i}\cdot\frac{1-e^{-P}}{P}\cdot\frac{d\big(W\cdot(\delta_{L,b}-\delta_x)\big)}{dt} \tag{7}$$

$$\delta_{L,e} = \delta^s_{L,e} - \frac{\alpha_k\alpha_{eq}r_t}{w_i}\cdot\frac{d\Big(W\cdot\frac{1-e^{-P}}{P}\cdot(\delta_{L,e}-\delta_x)\Big)}{dt} \tag{8}$$

where P is the Péclet number. In the limit of $P\to 0$, Eqns (7) and (8) reduce to $\delta_{L,e} = \delta_{L,b}$ or the well mixed condition. F05 allows W to vary with time. If W is also held constant, this model becomes identical to D74.

Big-leaf Model and Parameterizations. A big-leaf photosynthesis/transpiration model (Ronda *et al.*, 2001) was employed to calculate the canopy evapotranspiration (ET), canopy temperature (T_c) and the resistance terms (r_a, r_b, and r_c). Different values were used for the C_3 wheat and C_4 corn for the plant physiological parameters including the mesophyll conductance, the initial light use efficiency, the CO_2 compensation point and the maximal primary productivity. The relative humidity referenced to canopy temperature (RH_c), the equilibrium fractionation factor (ε_{eq}), and the apparent kinetic fractionation factor (ε_k), input variables required by the three isotopic submodels (Fig. 1), were then determined from the big-leaf model outputs.

The integrated model system was driven by observed meteorological and plant morphological variables. The input data common to the three isotopic models are the $H_2{}^{18}O$ composition of atmospheric water vapor (δ_a) and that of xylem water (δ_x). D74 and F05 also require data on W. A seasonal time series of W was established by linear interpolation between the weekly W measurements. Superimposed on the seasonal variation was a diurnal variation according to the diurnal composite W measured during the intensive periods. The input data of the big-leaf model include micrometeorological variables (air temperature, relative humidity, solar radiation, sky longwave radiation, atmospheric CO_2 concentration, wind speed, and friction velocity), soil temperature and moisture, leaf area index (LAI), and canopy height.

Tunable parameters of the model were optimized according to the observed latent heat flux and the foliage ^{18}O content. The big-leaf model contains two tunable parameters in the stomatal resistance parameterization, the vapor pressure deficit constant D_0 and the CO_2 concentration constant a_1 in eqn (11) of Ronda *et al.* (2001). They were tuned by a nonlinear least squares method to minimize the difference between the observed and the simulated latent heat flux. The optimization results were $D_0 = 0.50$ kPa and $a_1 = 11.9$ for wheat and $D_0 = 0.74$ kPa and $a_1 = 4.2$ for corn, using the complete dataset for each crop. The one free isotopic parameter L_{eff}, the effective length in the Péclet number in F05, was tuned with the observed $\delta_{L,b}$; the optimized value was essentially zero ($L_{eff} = 2.3 \times 10^{-9}$ m) for both wheat and corn.

Results

Leaf water content (W) is an important determinant of the non-steady state behavior of δ_L. The midday W decreased continuously from the early to the late growth season for both wheat and corn, and was low in midday and high in the early morning (Fig. 2). During the wheat season, the midday W decreased from 11.2 mol m^{-2} (mol water per m^2 leaf area) on DOY 97 to 7.5 mol m^{-2} (DOY 154), with a seasonal total decline of 3.7 mol m^{-2}. During the corn season, the midday W decreased from 12.3 mol m^{-2} (DOY 195) to 7.4 mol m^{-2} (DOY 246), with a change of 4.9 mol m^{-2}. Measurements during the four intensive periods show that the day-to-night variation of wheat W ranged from 0.3 (DOY 144) to 1.1 mol m^{-2} (DOY 142), with a mean value of about 0.5 mol m^{-2}, and that of corn W ranged from 0.8 (DOY 245) to 1.5 mol m^{-2} (DOY 244), with a mean value of 1.1 mol m^{-2}. Thus both the seasonal and diurnal variations in W were smaller for wheat than for corn.

A notable feature is that the diurnal variations in wheat $\delta_{L,b}$ were smaller than those in corn $\delta_{L,b}$ (Fig. 3). The 24 h, midday (10:00–15:00 LST) and midnight (22:00–3:00 LST) mean values of the observed $\delta_{L,b}$ during the intensive periods were 2.7, 4.2, and 1.6‰ for wheat leaves, respectively, and 2.9, 8.0, and 0.1‰ for corn leaves, respectively, showing that the canopy

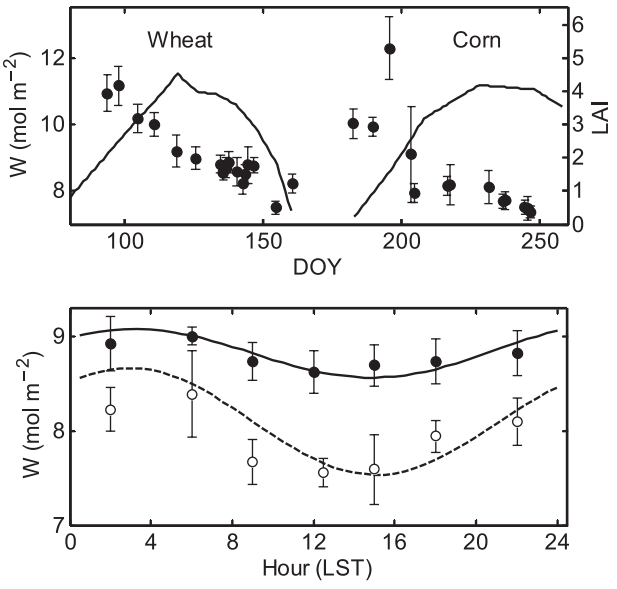

Fig. 2 Top panel: leaf water content (W, mol m^{-2} leaf area, closed circles) observed in midday and leaf area index (LAI, solid lines). Bottom panel: diurnal composite W observed during the intensive sampling periods for wheat (closed circles) and corn (open circles) and sinusoidal curve fits. Error bars are ±1 standard deviation of four spatial replicates.

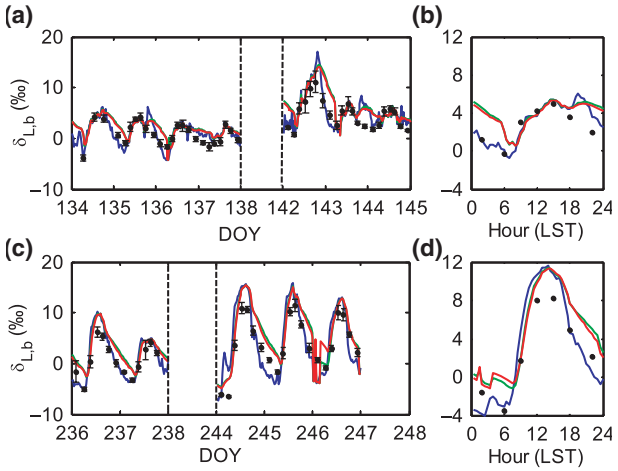

Fig. 3 Time series (a: wheat; c: corn) and ensemble diurnal patterns (b: wheat; d: corn) of the observed and simulated canopy mean values of $\delta_{L,b}$ during the intensive periods (blue line, C65; green line, D74; red line, F05; closed circles, observations). Mean values of the xylem and water vapor isotopic compositions during the intensive periods were −6.9‰ and −11.5‰ for wheat and −8.5‰ and −15.2‰ for corn. Error bars are ±1 standard deviation of four spatial replicates.

mean $\delta_{L,b}$ of wheat was lower in midday and higher at night in comparison to that of corn, while the 24 h mean value of wheat was lower. For reference, the mean values of δ_x and δ_a were −6.8 and −11.5‰ during the wheat intensive periods, and −8.5 and −15.2‰ during the corn intensive periods, respectively.

The observed diurnal variations were reproduced reasonably well by the three models (Figs 3 and 4), both on days with strongly diurnal variations (e.g., DOY 142) and on days that lacked variations (e.g., DOY 137 and 144). C65 slightly outperformed F05 and D74 in the simulation of the nighttime $\delta_{L,b}$. The three models produced nearly identical results for the midday periods; the simulated midday $\delta_{L,b}$ was 4.4‰, 4.3‰, and 4.2‰ for wheat and 10.5‰, 9.8‰, and 9.6‰ for corn

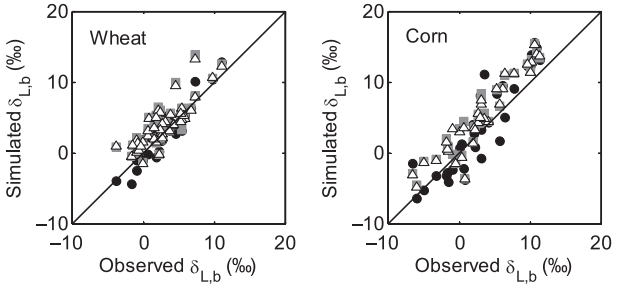

Fig. 4 Scatter plot of the modeled $\delta_{L,b}$ against the observations during wheat and corn intensive periods (closed circles: C65; squares: D74; triangles: F05).

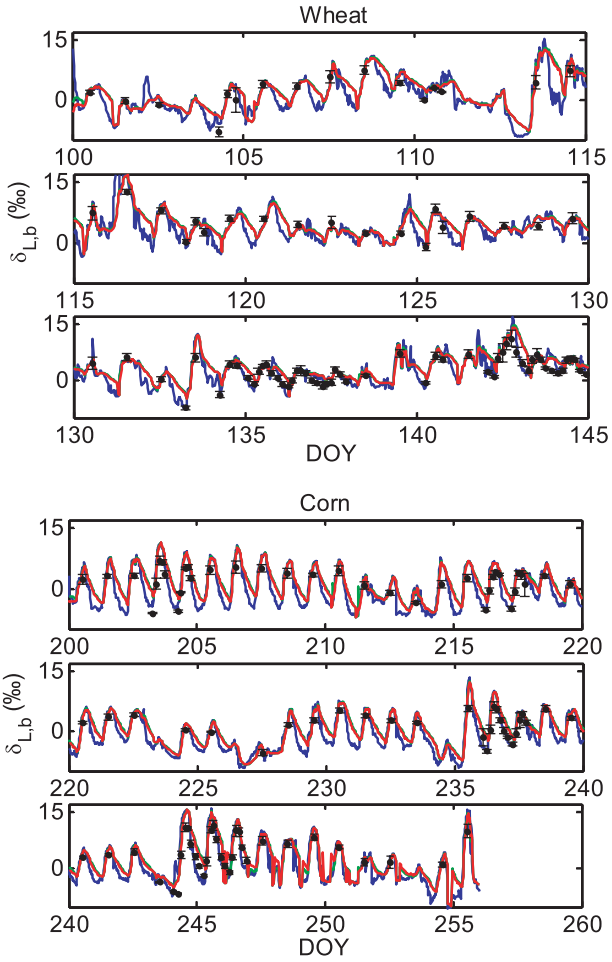

Fig. 5 Time series of the observed and simulated $\delta_{L,b}$ in wheat and corn canopy over the growing seasons (blue line, C65; green line, D74; red line, F05 model; closed circles, observation). Error bars are ±1 standard deviation of four spatial replicates.

according to C65, D74 and F05, respectively. Larger differences were found in the simulated midnight $\delta_{L,b}$, with mean values of 2.1‰, 4.7‰, and 4.4‰ for wheat and −2.0‰, 1.7‰, and 1.3‰ for corn according to C65, D74, and F05, respectively.

The three models also captured the seasonal variations (Fig. 5). Our measurement is among the few made on the seasonal time scale in the published literature (Welp *et al.*, 2008; Wingate *et al.*, 2010; Griffis *et al.*, 2011; Kim, 2011). The mean model bias errors (ME) were less than 2.0‰, the root mean squares deviation (RMSD) less than 2.6‰ and index of agreement (IA) better than 0.90 (Table 2).

A summary of statistics on the model-predicted $\delta_{L,b}$ for the two crop seasons over three averaging periods (24 h, midday, and midnight) is shown in Table 3. Consistent with the results shown in Fig. 3, the difference among the three models mainly occurred at night, with the F05 and D74 predictions about 2.5‰ higher than the C65 prediction.

The model-to-model biases occurred primarily at night (18:00–06:00 LST) and between the steady state model C65 and the non-steady state models D74 and F05 (Fig. 6). Since the turnover time of leaf water was much longer at night (midnight average τ = 8.2 and 6.3 h for wheat and corn, respectively) than in the daytime (τ = 0.5 and 0.8 h), it took longer time for the leaf water to reach steady state, and therefore the effects of non-steady state on isotopic enrichment were more significant at night than during the day. The bias between F05 and D74 was negligible.

Our model simulations confirm the need to consider turbulent diffusion when calculating the canopy-scale foliage water ^{18}O enrichment (Fig. 8). The apparent kinetic factor described by Eqn (3) is a canopy-scale property; it considers the different fractionation strengths associated with molecular and turbulent diffusion along the water vapor diffusion pathway (from the stomatal cavity to the atmospheric surface layer outside the canopy; Lee *et al.*, 2009). For wheat, if the aerodynamic resistance r_a was omitted in the apparent kinetic fractionation parameterization, the simulated $\delta_{L,b}$ was obviously biased high for all the models. For example, the F05 midday mean value of $\delta_{L,b}$ increased to 9.6‰ from the original 4.9‰. A similar model sensitivity has been shown for a soybean canopy (Xiao *et al.*, 2010). Model performance for corn was less sensitive to the apparent kinetic fractionation formulation; omission of r_a increased the midday F05 prediction by 1.1‰.

Table 2 The index of agreement (IA), root mean square deviation (RMSD), and mean error (ME) of the three model schemes over the two crop seasons

		C65			D74			F05		
Crop	Period	IA	RMSD (‰)	ME (‰)	IA	RMSD (‰)	ME (‰)	IA	RMSD (‰)	ME (‰)
Wheat	Whole day	0.95	1.6	0.4	0.90	2.1	1.0	0.91	2.0	1.0
	Nighttime	0.88	1.8	1.0	0.73	3.6	3.3	0.75	3.3	3.0
Corn	Whole day	0.92	2.6	1.6	0.91	2.6	2.0	0.92	2.5	1.9
	Nighttime	0.83	2.4	−1.7	0.76	3.5	2.3	0.80	3.0	1.8

Table 3 A summary of statistics on the model-predicted $\delta_{L,b}$ (‰) for the two crop seasons over three averaging periods [24 h, midday (10:00–15:00 LST) and midnight (22:00–3:00 LST)]. For reference, the mean xylem and water vapor isotopic compositions were −6.9‰ and −12.8‰ for wheat and −8.2‰ and −15.6‰ for corn, respectively.

	Wheat			Corn		
	C65	D74	F05	C65	D74	F05
24 h	2.3	3.3	3.2	−0.1	1.1	1.0
Midday	4.3	4.2	4.1	4.6	4.1	4.0
Midnight	1.0	3.4	3.1	−3.4	−0.6	−0.9

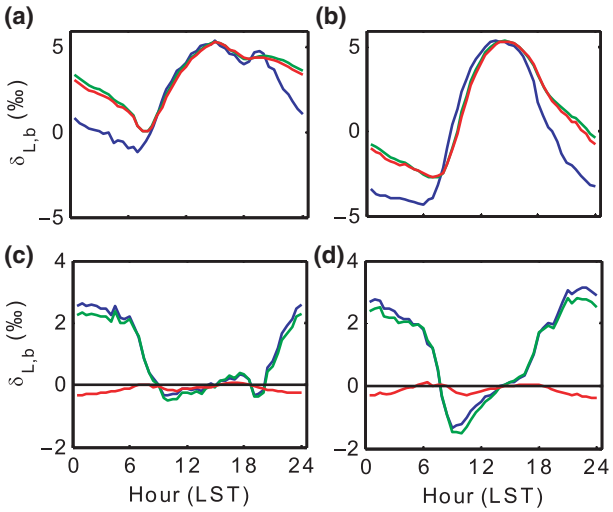

Fig. 6 Top panels: diurnal composite of the modeled $\delta_{L,b}$ for wheat (a) and corn growing season (b) (blue line: C65, green line: D74; red line: F05); Bottom panels: difference among the three models for wheat (c) and corn (d) (blue line: D74 vs. C65; green line: F05 vs. C65; red line: F05 vs. D74).

Discussion

Differences among the Three Models

Comparison of the three models of varying complexity (Table 1) allows us to differentiate the roles of various isotopic mechanisms underlying the observed variations. The relevant mechanisms include kinetic fractionation, leaf water turnover, time variations in *W* and the Péclet effect. With the inclusion of turbulent diffusion in the apparent kinetic fractionation formulation, all the three models captured reasonably well the observed seasonal variations of midday δ_L (Fig. 5 and Table 2). Numerous leaf- and canopy-scale studies have documented the effect of non-steady state (e.g., Farquhar & Cernusak, 2005; Lai *et al*., 2006; Seibt *et al*., 2006; Welp *et al*., 2008; Wingate *et al*., 2010; Griffis *et al*., 2011), the Péclet effect (Gan *et al*., 2002, 2003; Barbour & Farquhar, 2004; Farquhar & Cernusak, 2005) and the effect of the leaf water turnover rate (Griffis *et al*., 2011) on leaf water ^{18}O enrichment. The modeling study of Xiao *et al*. (2010) suggests that for soybean the Péclet effect is less important to the leaf water ^{18}O enrichment than the effect of non-steady state at the canopy scale. In this study, the optimized value of the scaled effective length L_{eff} in the Péclet number was essentially zero for both the wheat and the corn ecosystem. The small L_{eff} implies that at the canopy scale the Pélect effect was negligible so the only difference between D74 and F05 is that D74 did not consider the time variations in *W* whereas F05 did (Table 1). A comparison between the two suggests that the *W* time variations played a minor role on leaf water enrichment; their omission would introduce errors of no more than 0.3‰ at night (Fig. 6) and no more than 0.1‰ when averaged over the 24 h cycle (Table 3). The convergence of the F05 and the D74 predictions confirms the necessity to consider the effect of leaf water turnover in modeling δ_L and supports the postulation that it is not necessary to deal with changes in *W* in field conditions (Farquhar & Cernusak, 2005).

The roles of turbulent diffusion and leaf water turnover were not symmetrical through the course of the day. Omission of turbulence in the apparent kinetic fractionation parameterization would cause overestimation of δ_L primarily in the daytime hours, whereas omission of the leaf water turnover would cause underestimation of δ_L at night and with little consequence for the daytime. According to our sensitivity test, if both were omitted (as in the leaf-scale Craig-Gordon model), these errors would largely cancel out when averaged over periods of the diurnal cycle or longer, with the seasonal mean δ_L changing by less than 1.1‰ in comparison to the F05 predictions. However the mean values are misleading because the diurnal amplitude of δ_L would increase by 1.3‰ and 1.6‰ for wheat and corn, respectively, in comparison to the F05 predictions shown in Fig. 5.

The negligible difference between D74 and F05 indicates that the implicit assumptions made by D74 – that the ^{18}O content is well mixed in leaf water and that *W* is invariant with time – are good approximations for canopy-scale applications. D74 has been used in regional and global scale models of atmospheric $C^{18}OO$ and $H_2{}^{18}O$ (Riley *et al*., 2002; Cuntz *et al*., 2003; Still *et al*., 2009). Although having a more rigorous treatment than D74 of the mass balance of the leaf water pool and having integrated the empirical knowledge about ^{18}O diffusion in the pool, F05 is more difficult to use in regional and global models because of the tunable parameter L_{eff} and the lack of information on the time variations in *W*. There are field measurements of *W* to

help constrain the isotopic turnover time in several ecosystems (White, 1989; Yakir, 1998; Lai *et al*., 2006; Lee *et al*., 2007; Seibt *et al*., 2007; Xiao *et al*., 2010). *W* can also be inferred from satellite imagery (Yilmaz *et al*., 2008). However, few studies have reported the variations of *W* at fine enough time scales required by F05 (Farquhar & Cernusak, 2005; Xiao *et al*., 2010; Fig. 2).

Biotic versus Abiotic Controls on δ_L

In the C65 model, abiotic influences on δ_L, such as RH_c and δ_a, are dealt with explicitly and biotic influences are realized through the alteration of the apparent kinetic fractionation factor by stomatal resistance (Farquhar *et al*., 1989). In the limit that kinetic fractionation is purely molecular, a situation equivalent to having either an infinite stomatal resistance or a negligibly small aerodynamic resistance, δ_L is constrained by two asymptotic values at low and high RH. Farquhar *et al*. (2007) show that $\delta_L - \delta_x$ should equal the sum of the molecular kinetic factor (28‰) and the equilibrium factor (~9‰) at $RH_c = 0$ and approximately zero at $RH_c = 1$, giving a theoretical humidity sensitivity of about −0.40‰/% RH change (see also Still *et al*., 2009). The sensitivity observed in this study was about half of this theoretical value (−0.20‰/% RH). Welp *et al*. (2008) also observed a low sensitivity (−0.27‰/% RH) for a soybean system. According to the authors' unpublished data, the sensitivity was −0.33‰/%RH for a temperate deciduous forest (Kim, 2011) and −0.25‰/% RH for a short steppe grassland (Wen *et al*., 2012). It appears that δ_L is more sensitive to RH for natural ecosystems with larger stomatal resistance than for managed cropland ecosystems. Calculations with an isotopic large-eddy simulation model show that the sensitivity may also depend on surface roughness (Lee *et al*., 2012).

The strong negative correlation with RH can explain the larger daily variations of $\delta_{L,b}$ in corn than in wheat during the intensive campaigns (Fig. 3). The RH_c diurnal variation was in the range of 31–96% for corn and of 44–96% for wheat. The larger RH variation in corn would result in a 3.7‰ larger variation in $\delta_{L,b}$.

Because a weighting scheme was used to adjusting the apparent kinetic fractionation factor (Eqn 3), leaves with higher stomatal resistance are generally more enriched in $H_2{}^{18}O$ under similar hydrological conditions (Wang & Yakir, 1995; Barbour & Farquhar, 2000; Helliker & Ehleringer, 2000). C_3 plants usually have lower stomatal resistance than C_4 plants (Pearcy & Ehleringer, 1984; Knapp, 1993). In this study, the midday mean value of the canopy resistance r_c was 0.8 m^2 s mol^{-1} for wheat and 2.8 m^2 s mol^{-1} for corn, respectively. The apparent kinetic fractionation factor ε_k of wheat was much lower than that of corn, with the midday mean values of 13.2 and 23.2‰, respectively. There were, however, negligible differences in the modeled seasonal mean δ_L between wheat and corn (Table 3). In other words, variations in abiotic conditions in the field can offset some or all of the stomatal effect.

The difference in canopy resistance contributed to the contrasting non-steady state behaviors between the two crops (Fig. 6). Largely because of the lower r_c, wheat had a shorter isotopic turnover time (0.5 h) than corn (0.8 h) in the midday periods. As a result, its departure from steady state, as measured by the difference between the F05 and C65 models, was lower than 0.5‰ from 08:00 to 20:30 LST. Using this threshold, corn did not attain steady state except for a shorter duration in the afternoon (12:30–16:30 LST). Our results suggest that the steady state assumption is a better approximation in the daytime than at night and for ecosystems with lower canopy resistance (Cernusak *et al*., 2002, 2008).

Leaf water content *W* is a prescribed biological parameter in D74 and F05. The *W* value varies within the range of 3.4–18.4 mol m^{-2} (projected leaf area) in the literature (Farquhar & Cernusak, 2005; Lee *et al*., 2007; Seibt *et al*., 2007; Xiao *et al*., 2010), with a mean of 8.9 ± 4.2 mol m^{-2} (number of ecosystems = 7, including the two crops in this study). These studies suggest that the deviation from steady state at night should be greater for plants with larger *W*. For example, Seibt *et al*. (2007) compare nocturnal δ_L between a beech and a sitka spruce ecosystem. Their beech leaves have a low *W* value of 3.4 mol m^{-2} (the lowest among the studies cited above), and the difference between the D74 and C65 predictions is about 2‰ at midnight. In comparison, the difference between the two predictions is greater than 10‰ for the sitka spruce leaves having a high *W* of 11.8 mol m^{-2}. Our *W* values fell between the values for their forests (Fig. 2) and the departure from steady state was approximately 3‰ at midnight (Fig. 6).

The modeled midday $\delta_{L,b}$ shows varying bias errors over the growing seasons (Fig. 5). The prediction errors do not seem to have stemmed from errors in the fractionation parameterizations because all the three submodels had similar biases. The bias of canopy temperature T_c simulation introduced errors in the wheat $\delta_{L,b}$ simulation (Fig. 7). The reader is reminded that T_c, an input variable to the isotopic submodels (Fig. 1), was solved from the surface energy balance equation in the standard LSM. A significant linear positive relationship was found between the bias of the T_c simulation and the bias of the $\delta_{L,b}$ simulation by F05 for both wheat (linear correlation $r = 0.32$, $P < 0.05$) and

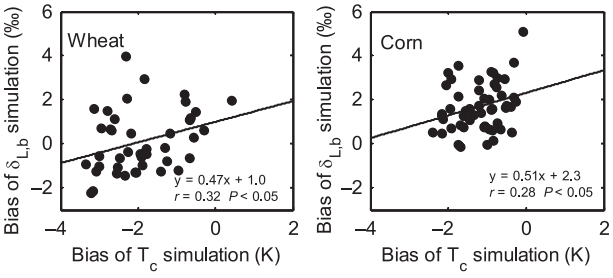

Fig. 7 Bias of the midday foliage ^{18}O composition ($\delta_{L,b}$) simulated by F05 vs. the bias of the simulated canopy temperature (T_c).

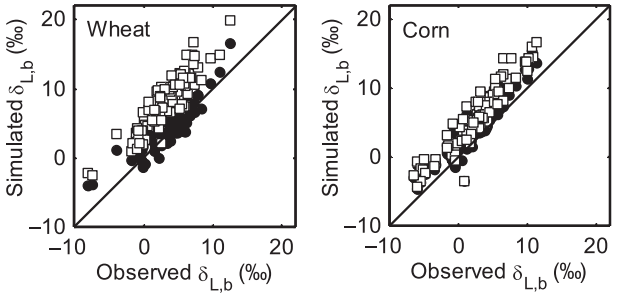

Fig. 8 Measured $\delta_{L,b}$ vs. $\delta_{L,b}$ simulated by F05 considering (closed circles) and omitting turbulent diffusion (squares) in the apparent kinetic fractionation formulation.

corn (r = 0.27, P < 0.05). Uncertainties in T_c is also a source of errors in $\delta_{L,b}$ simulated with the same isotopic LSM for a soybean ecosystem (Xiao *et al*., 2010). A low bias in T_c caused RH to increase which would decrease $\delta_{L,b}$.

Leaf Scale versus Canopy Scale

The mean δ^{18}O of foliage water at the canopy scale behaved in manners that were mostly predictable according to the mechanistic knowledge established by leaf- and plant-scale research. The large departure from steady state in the evening (Figs 3 and 6), the dominant role of RH and good accuracy of the C65 model in midday (Figs 3 and 5) are well-known features of δ_L at the leaf scale. However, this result is not intuitive given the large spatial variations in δ_L within the canopy layer (Appendix A). For example, it was common that the δ_L in the upper and lower canopy layers would differ by 5‰ in midday. Still larger variations were seen with leaf position: the base-to-tip gradient of the corn leaves could reach 15‰, a variation that was comparable to the temporal variations of the canopy mean δ_L over the whole growing season (Fig. 5). This last example is particularly noteworthy. Helliker & Ehleringer (2000) show that the Craig-Gordon model does not work for grass leaves because of a "string-of-lakes" effect or progressive enrichment along the parallel veins of these leaves. These large micro-scale "noises" were filtered out by our field sampling scheme (section on Materials and Methods) such that the δ_L values reported herein represented the algebraic mean across canopy and leaf positions. (Spatial replication further reduced the variability.) That the canopy δ_L was mostly predictable according to the Craig-Gordon model (Figs 3 and 5) while the microscale δ_L is not (Helliker & Ehleringer, 2000) suggests some strong compensation mechanism at the canopy scale.

The success of the δ_L models was helped by the canopy-scale apparent kinetic fractionation formulation (Fig. 8). A distinction between the canopy and the leaf scale is that the former involves turbulent diffusion in the atmospheric surface layer whereas the latter does not. Our results show that after turbulent diffusion has been accounted for in the apparent kinetic factor parameterization (Eqn 3), the leaf-scale enrichment models can be applied to the canopy scale with good accuracy. The effect of turbulent diffusion was stronger for wheat, which had lower canopy resistance, than for corn. We postulate that in global modeling studies the canopy-scale apparent kinetic formulation will improve model performance especially for productive ecosystems which generally have low canopy resistance.

The notion of the Péclet effect is, however, not transferable from the leaf scale to the canopy scale. At the leaf scale, this effect describes the process in which the $H_2{}^{18}O$ molecules diffuse, in the opposite direction of the mass flow of water, from the site of evaporation within the leaf to the less enriched water near the veins (Farquhar & Lloyd, 1993). At the canopy scale, however, the $H_2{}^{18}O$ molecules in the more enriched leaves (such as in the upper canopy at midday, Appendix A) cannot move via molecular diffusion to the less enriched leaves in another part of the canopy. This scale incomparability may be one reason why the canopy-scale version of the F05 model was forced to have a very small Péclet number. Thus, we are left with a paradoxical situation: The model implies a well mixed foliage water pool whereas the observations show that this pool was clearly stratified within the canopy (Appendix A). Overcoming this paradox will require more sophisticated multilayer models (Baldocchi, 1992; Leuning, 1995; de Pury & Farquhar, 1997; Ogée *et al*., 2003) than the simple big-leaf model used in this study.

The high model biases for corn (Figs 3 and 5) could have resulted from the simple upscaling schemes used both in the field measurement and in the models. Our leaf sampling strategy was meant to obtain the mean canopy $^{18}O/^{16}O$ ratio. In the case of corn, the samples were even mixture of small leaf segments taken at the

base, middle, and tip of a selected leaf. The modeling study of Farquhar & Gan (2003) suggests that this method may have underestimated the true average because the $H_2{}^{18}O$ distribution with leaf position is not linear. In the LSM, the leaf photosynthesis and stomatal resistance were weighted by photosynthetically active radiation with a fixed canopy light extinction coefficient of 0.6. Unlike multi-layer and two-leaf models (de Pury & Farquhar, 1997), this scaling method is incapable of handling the interaction between stomatal behavior and leaf-scale humidity variations in the canopy. Strictly speaking, there is a fundamental difficulty in interfacing the two-leaf model with the isotopic parameterizations. This is because mass balance requires that we track the time rate of changes of both ^{18}O and ^{16}O masses in a *fixed set* of foliage (as in Eqn 7), but the fractions of sunlit and shaded leaves are variable with solar elevation. Now that the results were found to be insensitive to the temporal variations in *W*, it is not necessary to consider the time rate of changes in the two-leaf model.

In leaf-scale studies, a number of other biotic factors are proved to be important in controlling the leaf water ^{18}O enrichment. Helliker & Ehleringer (2000) report that leaf water ^{18}O enrichment of C_4 grasses is greater than that of C_3 grasses under controlled conditions; They attribute this to interveinal differences between the two functional groups. The modeling study of Ogée *et al.* (2007) suggests that it is the difference in mesophyll tortuosity between C_3 and C_4 plants rather than in leaf length or interveinal distance that contributes to the stronger enrichment in C_4 leaves than in C_3 leaves. Our big-leaf model does not consider these morphological traits through mathematical parameterizations.

Implications for Global Change Studies

The $\delta^{18}O$ of foliage water is an important determinant of atmospheric $O^{18}O$ and $C^{18}OO$ budgets. The classic theories of the Earth Dole effect (Bender *et al.*, 1994) and vegetation effects on atmospheric $C^{18}OO$ (Farquhar *et al.*, 1993) have relied on the simple Craig-Gordon model for the δ_L calculation. That C65 performed equally well in daylight hours as the more sophisticated D74 and F05 suggests that the steady state assumption is acceptable for determining the photosynthetic $O^{18}O$ and $C^{18}OO$ fluxes at the canopy scale. Perhaps these theories can be improved by incorporating a variable, rather than a constant, kinetic fractionation factor. Since more productive ecosystems generally have lower canopy resistance r_c and the apparent kinetic factor decreases with decreasing r_c, this approach may alter the regional distributions of $O^{18}O$ and $C^{18}OO$ by reducing the contributions of cropland and native vegetation in warm and wet climates and increasing those in dry and cool climates.

For partitioning the net ecosystem CO_2 flux into its gross component fluxes, ^{18}O is a useful tracer. Flux partitioning is of interest to global change scientists because the eddy covariance technique can only measure the net flux but validation of carbon flux models requires data on the component fluxes. The ^{18}O content of foliage respiration in the dark is extremely sensitive to δ_L and is much more enriched (Cernusak *et al.*, 2004) than that of soil respiration (e.g., Wingate *et al.*, 2010; Santos *et al.*, 2011). Incorporating the non-steady behaviors in the δ_L calculation (Fig. 6) will further increase the difference between the two isotopic end members.

Acknowledgements

We thank the three journal reviewers whose comments have improved this article. This study was supported by the National Basic Research Program of China (grant 2010CB833501), the National Natural Science Foundation of China (grants 30970517, 31070408 and 31100359), the Strategic Program of Knowledge Innovation of the Chinese Academy of Sciences (grant KZCX2-EW-QN305), the U. S. National Science Foundation (grant ATM-0914473), the Ministry of Education of China (grant PCSIRT), NUIST scientific foundation (grants KLME1006 and 20100357) and the Jiangsu Provincial Government (grant PAPD).

References

Baldocchi DD (1992) A Lagrangian random walk model for simulating water vapor, CO_2 and sensible heat flux densities and scalar profiles over and within a soybean canopy. *Boundary-layer Meteorology*, **61**, 113–144.

Barbour MM (2007) Stable oxygen isotope composition of plant tissue: a review. *Functional Plant Biology*, **34**, 83–94.

Barbour MM, Farquhar GD (2000) Relative humidity- and ABA-induced variation in carbon and oxygen isotope ratios of cotton leaves. *Plant, Cell and Environment*, **23**, 473–485.

Barbour MM, Farquhar GD (2004) Do pathways of water movement and leaf anatomical dimensions allow development of gradients in $H_2{}^{18}O$ between veins and the sites of evaporation within leaves? *Plant, Cell and Environment*, **27**, 107–121, doi: 10.1046/j.0016-8025.2003.01132.x.

Barbour MM, Fischer RA, Sayre KD, Farquhar GD (2000) Oxygen isotope ratio of leaf and grain material correlates with stomatal conductance and grain yield in irrigated wheat. *Australian Journal of Plant Physiology*, **27**, 625–637.

Bariac T, Rambal S, Jusserand C, Berger A (1989) Evaluating water fluxes of field-grown alfalfa from diurnal observations of natural isotope concentrations, energy budget and ecophysiological parameters. *Agricultural and Forest Meteorology*, **48**, 263–283.

Bender M, Sowers T, Labeyrie L (1994) The Dole effect and its variations during the last 130,000 years as measured in the Vostok ice core. *Global Biogeochemical Cycles*, **8**, 363–376.

Cernusak LA, Pate JS, Farquhar GD (2002) Diurnal variation in the stable isotope composition of water and dry matter in fruiting *Lupinus angustifolius* under field conditions. *Plant, Cell and Environment*, **25**, 893–907, doi: 10.1046/j.1365-3040.2002.00875.x.

Cernusak LA, Farquhar GD, Wong SC, Stuart-Williams H (2004) Measurement and interpretation of the oxygen isotope composition of carbon dioxide respired by leaves in the dark. *Plant Physiology*, **136**, 3350–3363.

Cernusak LA, Farquhar GD, Pate JS (2005) Environmental and physiological controls over oxygen and carbon isotope composition of Tasmanian blue gum, *Eucalyptus globulus*. *Tree Physiology*, **25**, 129–146.

Cernusak LA, Mejia-Chang M, Winter K, Griffiths H (2008) Oxygen isotope composition of CAM and C_3 *Clusia* species: non-steady-state dynamics control leaf water

^{18}O enrichment in succulent leaves. *Plant, Cell and Environment*, **31**, 1644–1662, doi: 10.1111/j.1365-3040.2008.01868.x.

Ciais P, Denning AS, Tans PP *et al.* (1997) A three-dimensional synthesis study of $\delta^{18}O$ in atmospheric CO_2 1. Surface fluxes. *Journal of Geophysical Research*, **102**, 5857–5872.

Craig H, Gordon LI (1965) Deuterium and oxygen-18 variations in the ocean and the marine atmosphere. In: *Proceedings of the Conference on Stable Isotopes in Oceanographic Studies and Paleotemperatures* (ed Tongiorgi E), pp 9–130. Laboratory of Geology and Nuclear Science, Pisa.

Cullen LE, Adams MA, Anderson MJ, Grierson PF (2008) Analyses of $\delta^{13}C$ and $\delta^{18}O$ in tree rings of *Callitris columellaris* provide evidence of a change in stomatal control of photosynthesis in response to regional changes in climate. *Tree Physiology*, **28**, 1525–1533.

Cuntz M, Ciais P, Hoffmann G, Knorr W (2003) A comprehensive global three-dimensional model of $\delta^{18}O$ in atmospheric CO_2: 1. Validation of surface processes. *Journal of Geophysical Research*, **108**, 4527.

Dole M, Lane GA, Rudd DP, Zaukelies DA (1954) Isotopic composition of atmospheric oxygen and nitrogen. *Geochimica et Cosmochimica Acta*, **6**, 65–78.

Dongmann G, Nürnberg HW, Förstel H, Wagener K (1974) On the enrichment of $H_2{}^{18}O$ in the leaves of transpiring plants. *Radiation and Environmental Biophysics*, **11**, 41–52.

Epstein S, Yapp C (1977) Isotope tree thermometers. *Nature*, **266**, 477–478.

Evans MN, Schrag DP (2004) A stable isotope-based approach to tropical dendroclimatology. *Geochimica et Cosmochimica Acta*, **68**, 3295–3305.

Farquhar GD, Cernusak LA (2005) On the isotopic composition of leaf water in the non-steady state. *Functional plant biology*, **32**, 293–303.

Farquhar GD, Gan KS (2003) On the progressive enrichment of the oxygen isotopic composition of water along a leaf. *Plant, Cell and Environment*, **26**, 801–819.

Farquhar GD, Lloyd J (1993) Carbon and oxygen isotope effects in the exchange of carbon dioxide between terrestrial plants and the atmosphere. In: *Stable Isotopes and Plant Carbon-water Relations* (eds Ehleringer JR, Hall AE, Farquhar GD), pp 47–70. Academic Press, San Diego.

Farquhar GD, Hubick KT, Condon AG, Richards RA (1989) Carbon isotope discrimination and plant water-use efficiency. In: *Stable Isotopes in Ecological Research*, Vol 68 (eds Rundel PW, Ehlerginger JR, Nagy KA), pp 21–40. Springer-Verlag, New York.

Farquhar GD, Lloyd J, Taylor JA *et al.* (1993) Vegetation effects on the isotope composition of oxygen in atmospheric CO_2. *Nature*, **363**, 439–443.

Farquhar GD, Cernusak LA, Barnes B (2007) Heavy water fractionation during transpiration. *Plant Physiology*, **143**, 11–18.

Flanagan LB, Ehleringer JR (1991) Effects of mild water-stress and diurnal changes in temperature and humidity on the stable oxygen and hydrogen isotopic composition of leaf water in *Cornus-Stolonifera* L.. *Plant Physiology*, **97**, 298–305.

Flanagan LB, Comstock JP, Ehleringer JR (1991) Comparison of modeled and observed environmental-influences on the stable oxygen and hydrogen isotope composition of leaf water in *Phaseolus-Vulgaris* L. *Plant Physiology*, **96**, 588–596.

Gan KS, Wong SC, Yong JWH, Farquhar GD (2002) ^{18}O spatial patterns of vein xylem water, leaf water and dry matter in cotton leaves. *Plant Physiology*, **130**, 1008–1021.

Gan KS, Wong SC, Yong JWH, Farquhar GD (2003) Evaluation of models of leaf water ^{18}O enrichment using measurements of spatial patterns of vein xylem water, leaf water and dry matter in maize leaves. *Plant, Cell and Environment*, **26**, 1479–1495.

Gray J, Thompson P (1976) Climatic information from $^{18}O/^{16}O$ ratios of cellulose in tree rings. *Nature*, **262**, 481–482.

Griffis TJ, Lee X, Baker JM *et al.* (2011) Oxygen isotope composition of evapotranspiration and its relation to C_4 photosynthetic discrimination. *Journal of Geophysical Research*, **116**, G01035, doi: 10.1029/2010JG001514.

Helliker BR, Ehleringer JR (2000) Establishing a grassland signature in veins: ^{18}O in the leaf water of C_3 and C_4 grasses. *Proceedings of the National Academy of Sciences of the United States of America*, **97**, 7894–7898.

Helliker BR, Richter SL (2008) Subtropical to boreal convergence of tree-leaf temperatures. *Nature*, **454**, 511–515, doi: 10.1038/nature07031.

Hoffmann G, Cuntz M, Weber C *et al.* (2004) A model of the Earth's Dole effect. *Global Biogeochemical Cycles*, **18**, GB1008, doi: 10.1029/2003GB002059.

Kahmen A, Sachse D, Arndt SK, Tu KP, Farrington H, Vitousek PM, Dawson TE (2011) Cellulose $\delta^{18}O$ is an index of leaf-to-air vapor pressure difference (VPD) in tropical plants. *Proceedings of the National Academy of Sciences of the United States of America*, **108**, 1981–1986.

Kim K (2011) *Laboratory and field investigations of stable water isotopes in ecosystems*. Unpublished PhD thesis, Yale University, New Haven. Available at: http://xle-elab.sites.yale.edu/publications (accessed 8 September 2011)

Knapp AK (1993) Gas exchange dynamics in C_3 and C_4 grasses: consequence of differences in stomatal conductance. *Ecology*, **74**, 113–123.

Lai C, Ehleringer JR, Bond BJ, Paw UKT (2006) Contributions of evaporation, isotopic non-steady state transpiration and atmospheric mixing on the $\delta^{18}O$ of water vapour in Pacific Northwest coniferous forest. *Plant, Cell and Environment*, **29**, 77–94.

Lee X, Kim K, Smith R (2007) Temporal variations of the isotopic signal of the whole-canopy transpiration in a temperate forest. *Global Biogeochemical Cycles*, **21**, GB3013, doi: 10.1029/2006GB002871.

Lee X, Griffis TJ, Baker JM, Billmark KA, Kim K, Welp LR (2009) Canopy-scale kinetic fractionation of atmospheric carbon dioxide and water vapor isotopes. *Global Biogeochemical Cycles*, **23**, GB1002, doi: 10.1029/2008GB003331.

Lee X, Huang J, Patton EG (2012) A large-eddy simulation study of water vapour and carbon dioxide isotopes in the atmospheric boundary layer. *Boundary-Layer Meteorology*, doi: 10.1007/s10546-011-9631-3.

Leuning R (1995) A critical appraisal of a combined stomatal-photosynthesis model for C_3 plants. *Plant Cell Environment*, **18**, 339–355.

Libby Pandolfi LJ, Payton PH, Marshall J III, Becker B, Giertz-Sienbenlist V (1976) Isotopic tree thermometers. *Nature*, **261**, 284–288.

Majoube M (1971) Fractionnement en oxygene-18 et en deuterium entre l'eau et sa vapeur. *Journal de Chimie et Physique*, **58**, 1423–1436.

Merlivat L (1978) Molecular diffusivities of $H_2{}^{16}O$, $HD^{16}O$ and $H_2{}^{18}O$ in gases. *Journal of Chemical Physics*, **69**, 2864–2871.

Miller DL, Mora CI, Grissino-Mayer HD, Mock CJ, Uhle ME, Sharp Z (2006) Tree-ring isotope records of tropical cyclone activity. *Proceedings of the National Academy of Sciences of the United States of America*, **103**, 14294–14297.

Ogée J, Brunet Y, Loustau D, Berbigier P, Delzon S (2003) *MuSICA*, a CO_2, water and energy multilayer, multileaf pine forest model: evaluation from hourly to yearly time scales and sensitivity analysis. *Global Change Biology*, **9**, 697–717.

Ogée J, Peylin P, Ciais P *et al.* (2004) Partitioning net ecosystem carbon exchange into net assimilation and respiration with canopy-scale isotopic measurements: an error propagation analysis with $^{13}CO_2$ and $CO^{18}O$ data. *Global Biogeochemical Cycles*, **18**, GB2019, doi: 10.1029/2003GB002166.

Ogée J, Cuntz M, Peylin P, Bariac T (2007) Non-steady-state, non-uniform transpiration rate and leaf anatomy effects on the progressive stable isotope enrichment of leaf water along monocot leaves. *Plant, Cell and Environment*, **30**, 367–387.

Pearcy RW, Ehleringer J (1984) Comparative ecophysiology of C_3 and C_4 plants. *Plant, Cell and Environment*, **7**, 1–13.

de Pury DGG, Farquhar GD (1997) Simple scaling of photosynthesis from leaves to canopies without the errors of big-leaf model. *Plant, Cell and Environment*, **20**, 537–557.

Riley WJ, Still CJ, Torn MS, Berry JA (2002) A mechanistic model of $H_2{}^{18}O$ and $C^{18}OO$ fluxes between ecosystems and the atmosphere: model description and sensitivity analyses. *Global Biogeochemical Cycles*, **16**, 1095, doi: 10.1029/2002GB001878.

Roden JS, Lin G, Ehleringer JR (2000) A mechanistic model for interpretation of hydrogen and oxygen isotope ratios in tree-ring cellulose. *Geochimica et Cosmochimica Acta*, **64**, 21–35.

Ronda RJ, de Bruin HAR, Holtslag AAM (2001) Representation of the canopy conductance in modeling the surface energy budget for low vegetation. *Journal of Applied Meteorology*, **40**, 1431–1444.

Santos EA, Wagner-Riddle C, Lee X *et al.* (2011) Use of the isotope flux ratio approach to investigate the $C^{18}O^{16}O$ and $^{13}CO_2$ exchange near the floor of a temperate deciduous forest. *Biogeosciences Discussion*, **8**, 7671–7712, doi: 10.5194/bgd-8-7671-2011.

Schultz NM, Griffis TJ, Lee X, Baker JM (2011) Identification and correction of spectral contamination in $^2H/^1H$ and $^{18}O/^{16}O$ measured in leaf, stem, and soil water. *Rapid Communications in Mass Spectrometry*, **25**, 3360–3368.

Seibt U, Wingate L, Berry JA, Lloyd J (2006) Non-steady state effects in diurnal ^{18}O discrimination by *Picea sitchensis* branches in the field. *Plant, Cell and Environment*, **29**, 928–939.

Seibt U, Wingate L, Berry A (2007) Nocturnal stomatal conductance effects on the $\delta^{18}O$ signatures of foliage gas exchange observed in two forest ecosystem. *Tree Physiology*, **27**, 585–595.

Sternberg L da SL (2009) Oxygen stable isotope ratios of tree-ring cellulose: the next phase of understanding. *New Phytologist*, **181**, 553–562.

Still CJ, Riley WJ, Biraud SC *et al.* (2009) Influence of clouds and diffuse radiation on ecosystem-atmosphere CO_2 and $CO^{18}O$ exchanges. *Journal of Geophysical Research*, **114**, G01018, doi: 10.1029/2007JG000675.

Treydte KS, Schleser GH, Helle G, Frank DC, Winiger M, Haug GH, Esper J (2006) The twentieth century was the wettest period in northern Pakistan over the past millennium. *Nature*, **440**, 1179–1182.

Walker CD, Leaney FW, Dighton JC, Allison GB (1989) The influence of transpiration on the equilibration of leaf water with atmospheric water-vapor. *Plant, Cell and Environment*, **12**, 221–234.

Wang X, Yakir D (1995) Temporal and spatial variations in the oxygen-18 content of leaf water in different plant species. *Plant, Cell and Environment*, **18**, 1377–1385.

Welp LR, Lee X, Kim K, Griffis TJ, Billmark KA, Baker JM (2008) $\delta^{18}O$ of water vapor, evapotranspiration and the sites of leaf water evaporation in a soybean canopy. *Plant, Cell and Environment*, **31**, 1214–1228.

Wen X, Lee X, Sun X, Wang J, Z Hu, Li S, Yu G (2012) Dew water isotopic ratios and their relations to ecosystem water pools and fluxes in a cropland and a grassland in China. *Oecologia*, **168**, 549–561, doi: 10.1007/s00442-011-2091-0.

West AG, Patrickson SJ, Ehleringer JR (2006) Water extraction times for plant and soil materials used in stable isotope analysis. *Rapid Communications in Mass Spectrometry*, **20**, 1317–1321, doi: 10.1002/rcm.2456.

White JWC (1989) Stable hydrogen isotope ratios in plants: a review of current theory and some potential applications. In: *Stable isotopes in ecological research*, Vol 68 (eds Rundel PW, Ehleringer JR, Nagy KA), pp 142–162. Springer-Verlag, Berlin.

Wingate L, Ogée J, Burlett R, Bosc A (2010) Strong seasonal disequilibrium measured between the oxygen isotope signals of leaf and soil CO_2 exchange. *Global Change Biology*, **16**, 3048–3064, doi: 10.1111/j.1365-2486.2010.02186.x.

Xiao W, Lee X, Griffis TJ, Kim K, Welp LR, Yu Q (2010) A modeling investigation of canopy-air oxygen isotopic exchange of water vapor and carbon dioxide in a soybean field. *Journal of Geophysical Research*, **115**, G01004, doi: 10.1029/2009JG001163.

Yakir D (1998) Oxygen-18 of leaf water: a crossroad for plant associated isotopic signal. In: *Stable Isotopes: Integration of Biological, Ecological and Geochemical Processes* (ed Griffiths H), pp. 147–168. BIOS Scientific Publishers Ltd, Oxford.

Yakir D, Sternberg LDL (2000) The use of stable isotopes to study ecosystem gas exchange. *Oecologia*, **123**, 297–311.

Yakir D, Berry JA, Giles L, Osmond CB (1994) Isotopic heterogeneity of water in transpiring leaves: identification of the components that controls the $\delta^{18}O$ of atmospheric O_2 and CO_2. *Plant, Cell and Environment*, **17**, 73–80.

Yilmaz MT, Hunt ER Jr, Jackson TJ (2008) Remote sensing of vegetation water content from equivalent water thickness using satellite imagery. *Remote Sensing of Environment*, **112**, 2514–1522.

Supporting Information

Additional Supporting Information may be found in the online version of this article:

Appendix S1. Observed Spatial and Temporal Variability of $\delta_{L,b}$

Appendix S2. Correction of IRIS Measurements for organic contamination

Table S1. Contamination correction to the $\delta^{18}O$ values of wheat and corn leaves and stems.

Figure S1. Spatial distribution of $\delta_{L,b}$ (‰) along the corn leaf at different times of the day, DOY 256.

Figure S2. The correlation between $\delta_{L,b}$ gradient (tip to base) in the corn leaves and relative humidity.

Figure S3. Observed midday (10:00–15:00 LST) $\delta_{L,b}$ in the upper (closed circles) and lower (open circles) canopy in wheat and corn. Error bars are ±1 standard deviation of four spatial replicates.

Figure S4. Time variation of $\delta_{L,b}$ during four intensive observation periods in the upper (closed circles) and lower layer of the canopy (open circles). Error bars are ±1 standard deviation of four spatial replicates.

Figure S5. Ethanol (a) and methanol (b) contamination correction curves for IRIS $\delta^{18}O$ measurement.

Figure S6. Comparison of IRIS and IRMS $\delta^{18}O$ measurements.

Please note: Wiley-Blackwell are not responsible for the content or functionality of any supporting materials supplied by the authors. Any queries (other than missing material) should be directed to the corresponding author for the article.